Journal of Clinical Laboratory Analysis

WILEY

RESEARCH ARTICLE OPEN ACCESS

Mitochondrial tRNA^{Glu} 14687A>G May Be A Novel Mutation for Type 2 Diabetes Mellitus

Xiaojuan Rao | Liran Xie | Shuangwei Shi | Yifan Fang

Department of Endocrinology, The Fifth Affiliated Hospital of Zhengzhou University, Zhengzhou, People's Republic of China

Correspondence: Xiaojuan Rao (raoxj888@sohu.com)

Received: 20 February 2025 | **Revised:** 22 April 2025 | **Accepted:** 6 May 2025

Funding: This work is supported by Medical Science and Technology Research Program of Henan Province, LHGJ20200474.

Keywords: Chinese pedigree | m.14687A>G mutation | mitochondrial dysfunction | mitochondrial tRNA^{Glu} | T2DM

ABSTRACT

Background: Sequence alternations in mitochondrial genomes, especially in mitochondrial tRNA (mt-tRNA), are closely related to type 2 diabetes mellitus (T2DM); however, the detailed molecular mechanism is still largely undetermined.

Methods: Herein, we reported a T2DM Chinese family by using molecular and biochemical analyses. The mtDNA mutations in this pedigree were detected by PCR and Sanger sequencing. Moreover, phylogenetic analysis was used to assess the pathogenic mitochondrial DNA (mtDNA) mutation. We further evaluated mt-tRNA stability levels and mitochondrial functions in cybrids with and without the m.14687A>G mutation.

Results: Members of this family expressed variable clinical phenotypes. Screening for the entire mitochondrial genomes revealed the occurrence of a novel m.14687A>G mutation, which was located at position 60 in the TψC loop of tRNA^{Glu}, and that position was important for tRNA structure and function. By establishing cybrids derived from three diabetic patients carrying the m.14687A>G mutation and three healthy individuals without this mutation, we noticed that this mutation caused approximately 52% reduction in tRNA^{Glu} stability level ($p < 0.0001$). The 14687G cybrid showed more severely impaired mitochondrial functions than the 14687A cybrid: mtDNA content, ATP, and mitochondrial membrane potential (MMP) and OXPHOS enzyme activities were markedly decreased. But the levels of reactive oxygen species (ROS) were significantly increased.

Conclusion: Our finding revealed that the novel m.14687A>G mutation resulted in aberrant mt-tRNA metabolism and mitochondrial dysfunctions, which should be regarded as a pathogenic mutation for T2DM.

1 | Introduction

Type 2 diabetes mellitus (T2DM) is a common health problem which affected approximately 10% of the total Chinese population [1]. The molecular basis of this disease is very complex; it has been widely accepted that T2DM can be caused by the combinations between personal lifestyle, genetic, as well as environmental factors [2]. In particular, insulin resistance (IR) plays a critical role in the pathogenesis of T2DM. It is defined as a relative impairment in the ability of insulin to exert its effects on glucose, protein, and lipid metabolism in target tissues. Increasing evidence suggested that IR has both heritable and environmental determinants centered on energy storage and metabolism [3]. Mitochondria use fat for energy production, and decreased mitochondrial function is associated with an increase in ectopic fat and IR. Resting ATP synthesis in skeletal muscle in IR subjects is reduced when compared with insulin sensitive individuals, suggesting a contribution of mitochondrial dysfunction to IR [4]. Moreover, mitochondrial malfunction and oxidative stress are inextricably linked, and both are strongly associated with IR and T2DM [5]. On the other hand, during ATP production, electrons are transferred from carriers in the electron transport chain Complex I through Complex IV, where these electrons

reduce oxygen to water [6]. Excessive ROS production will reduce mitochondrial function and subsequently generate more ROS in a vicious cycle, attenuate insulin action in adipocytes and myotubes [7], and abolish insulin-stimulated GLUT4 translocation in 3T3L1 cells by interfering with the insulin-mediated redistribution of IRS-1 and PI3-kinase [8, 9]. Thus, exploring the molecular mechanism underlying mitochondrial dysfunction-induced IR and T2DM is critical for understanding its pathophysiology.

Furthermore, maternally transmitted T2DM has been identified in several pedigrees, indicating that mtDNA mutations are important contributors to this disorder [10]. The well-known 3243A>G is the most frequent T2DM related mutation [11, 12]. In addition, some studies suggested that $tRNA^{Gly}$ 10,003T>C [13]; $tRNA^{Thr}$ 15897G>A [14]; $tRNA^{Trp}$ 5514A>G; and $tRNA^{Ser(AGY)}$ 12237C>T [15] mutations were involved in the progression of T2DM in several Chinese pedigrees. These mtDNA mutations occur in heteroplasmic forms and exhibit variability in clinical manifestation [16]. Nevertheless, the molecular mechanism underlying diabetes is still elusive.

Herein, we report the clinical, genetic, molecular, and biochemical characteristics of one Han Chinese family with T2DM. Molecular and genetic analyses revealed the presence of a novel $tRNA^{Glu}$ 14687A>G mutation, which was only found in matrilineal relatives but was absent in controls. To investigate the impacts of the m.14687A>G mutation on mitochondrial function, we evaluated tRNA steady-state levels, mtDNA copy number, ATP, MMP, ROS, and enzymatic activities of OXPHOS in trans-mitochondrial cybrid cells from three T2DM patients and controls with and without the m.14687A>G mutation.

2 | Materials and Methods

2.1 | Pedigrees Information

We enrolled a pedigree via the Department of Endocrinology, the Fifth Affiliated Hospital of Zhengzhou University (Figure 1). In addition, 180 age- and sex-matched healthy subjects (80 males and 100 females, ranged from 40 to 56 years, with an average age of 48) were enrolled in this study. Informed consent was obtained from the Ethics Committee of the Fifth Affiliated Hospital of Zhengzhou University (Approval No: KY2023088-K02). Moreover, the written informed consent was obtained from all participants attending for this study.

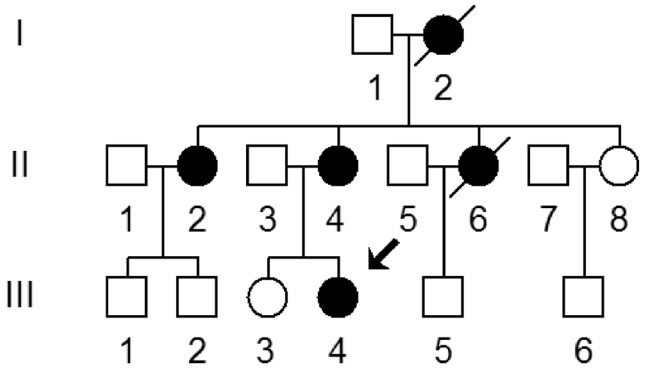

FIGURE 1 | One Han Chinese families with T2DM, arrow denoted the proband.

Clinically, diagnosis of diabetes was according to the guidelines of the American Diabetes Association: [17] (1) 0-h plasma glucose concentration ≥ 7.0 mmol/dL; (2) oral glucose tolerance test (OGTT) test: 2-h plasma glucose concentration ≥ 11.1 mmol/L; (3) the level of hemoglobin A1c (HbA1c) ≥ 6.5%.

2.2 | Risk Factors Assessments

A questionnaire was used to record the demographics, family history, and personal information of each participant who participated in our study. Body mass index (BMI), an estimate of total body fat, was defined as weight (kg) divided by the height in metres [18]. Blood pressure (BP) was assessed by an electronic sphygmomanometer, according to the protocol as previously described [19]. Hypertension was defined as a systolic BP ≥ 140 mmHg or the diastolic BP ≥ 90 mmHg [20]. The pure tone audiometric (PTA) examination was carried out according to a previous study [21]. Notably, the degree of deafness was dependent on the following criteria: normal hearing, < 20 dB (dB); mild, 21–40 dB; moderate, 41–70 dB; severe, 71–95 dB; profound, > 95 dB. In addition, vision acuity (VA) was assessed to determine the degree of visual loss: normal > 0.3, mild = 0.3–0.1, moderate < 0.1–0.05, severe < 0.05–0.02, profound < 0.02 [22].

Blood samples were collected from each participant after overnight fasting. Biochemical test related parameters were analyzed using standard laboratory methods (Hitachi, Tokyo, Japan). Fasting insulin (FINS) levels were analyzed using a chemiluminescent immunometric assay (IMMULITE; Siemens). The IR was evaluated as the homeostasis model assessment of IR (HOMA-IR) index, HOMA-IR = (FINS [μU/mL] × FBG [mmol/L])/22.5. Its value ≥ 2.69 was considered as IR [23].

2.3 | Mutations Analysis

We screened mitochondrial genome mutations in matrilineal relatives (II-2, II-4, and III-4) by using 24 primers, as described elsewhere [24]. The PCR products were then sequenced by the Sanger approach; subsequently, the sequence results were compared with the revised Cambridge Reference Sequence (rCRS, GenBank Accessible Number: NC_012920.1) [25]. Furthermore, the classification of the mitochondrial haplogroup was based on a phylogenetic tree, as previously described [26].

2.4 | Conservation Analysis

Phylogenetic analysis was performed to assess the pathogenic roles of mtDNA mutations. A total of 13 species were used for conservation analysis as described in a recent study [27]. We compared human mtDNA at a position to determine the level of conservation index (CI). A CI ≥ 75% was considered to indicate functional significance [28].

2.5 | Generation of Cybrid Cells

Infection of cells with Epstein–Barr virus can lead to proliferation and immortalization, resulting in the establishment of lymphoblastoid cell lines (LCLs) [29]. LCLs were derived from three patients (II-2, II-4, and III-4) with the m.14687A>G mutation, as well as three control subjects (C-1, C-2, and C-3) without this mutation who were cultured in RPMI 1640 medium, supplied with 10% FBS. These control subjects were healthy individuals and did not harbor the m.14687A>G mutation, nor did they have any family history of mitochondrial diseases such as diabetes, cardiovascular or neurological disease, or hearing loss.

2.6 | Northern Blot Analysis

To determine whether the m.14687A>G mutation influenced tRNA metabolism, the tRNA steady-state levels were examined by Northern Blot. The total RNA was first extracted from cybrid cell lines using a Ambion's TOTALLY RNA kit (Thermo Fisher, Shanghai); the Northern Blot was performed as described elsewhere [30]. The sequences for digoxigenin (DIG)-labeled probes specific to $tRNA^{Glu}$, $tRNA^{Met}$, $tRNA^{Cys}$ and 5S rRNA were: 5′-ATT CTC GCA CGG ACT ACA ACC ACG ACC AAT-3′; 5′-TAG TAC GGG AAG GGT ATA ACC AAC ATT TTC-3′; 5′-CCC CGG CAG GTT TGA AGC TGC TTC TTC GAA-3′; 5′-CTA ATT AAT TAT AAG GCC AGG ACC AAA CCT-3′, respectively.

2.7 | mtDNA Copy Number Analysis

The peripheral blood mtDNA copy number was assessed using real-time PCR in three patients with T2DM (II-2, II-4, and III-4) and three controls (C-1, C-2, and C-3), as described in a previous study [31]. Primers for amplification of the *ND1* gene were: forward 5′-AAC ATA CCC ATG GCC AAC CT-3′; reverse 5′-AGC GAA GGG TTG TAG TAG CCC-3′. Primers for amplification of β-globin were: forward 5′-GAA GAG CCA AGG ACA GGT AC-3′; reverse 5′-CAA CTT CAT CCA CGT TCA CC-3′. PCR was carried out in a final volume of 10 μL reaction mixture containing 1 μL DNA template (10 ng), 4 μL SYBR Green PCR Master Mix, 0.2 μL of each primer (10 mM) and 4.6 μL H_2O. The reactions were performed in triplicate using an ABI 7500 Fast Real-time PCR System (Applied Biosystems, CA) (SYBR Green Assay, Applied Biosystems).

2.8 | Analysis of ATP Production

ATP productions in cybrid cells were measured by using the CellTiter-Glo luminescent cell viability assay (Promega, G7572), according to the manufacturer's instructions [32]. Briefly, the assay buffer and substrate were equilibrated at room temperature, transferred to, and gently mixed with the substrate to obtain a homogeneous solution. After a 30-min equilibration of the cell plate at room temperature, 100 μL of the assay reagents were added into each well with 2×10^4 cells, and the content was mixed for 2 min on an orbital shaker to induce cell lysis. After 10-min incubation in room temperature, the luminescence was read on a microplate reader (Syneregy H1, BioTek).

2.9 | MMP Measurement

The JC-10 MMP microplate assay kit (Abcam, ab112134) was used according to previously described protocols [33]. Approximately 2×10^6 cells of each cybrid cell line were harvested, resuspended in 200 μL JC-10 Assay buffer, and then incubated at 37°C for 30 min. Alternatively, harvested cells were preincubated with 10 μM of FCCP for 30 min at 37°C prior to staining with JC-10 dye. After washing with PBS twice, cells were resuspended in 200 μL PBS. The fluorescent intensities for both J-aggregates and monomeric forms of JC-10 were measured at Ex/Em = 490/529 and 490/590 nm with a DB-LSR II flow cytometer system (Beckton Dickson Inc.).

2.10 | ROS Assessment

A total of 5×10^4 cells were resuspended in PBS to a final volume of 100 μL. The cells were then incubated with 10 μM of 2′,7′-dichloro dihydrofluorescein diacetate (DCFH-DA) for 30 min at 37°C in the dark. Following incubation, the cells were washed twice with PBS to remove excess DCFH-DA. Subsequently, the cells were seeded into a 96-well plate (Thermo M33089) under dark conditions to prevent any photobleaching of the fluorescent signal. The fluorescence intensity of each well was measured using a spectrofluorometer (FL×800, BioTek) at excitation and emission wavelengths of 485 nm and 535 nm, respectively, as previously described [34].

2.11 | Analysis of the Enzymatic Activities of OXPHOS Complexes

The enzymatic activities of Complex I ~ IV in control and mutant cells were measured as described elsewhere [35]. In short, for assessment of rotenone-sensitive Complex I activity, malonate-sensitive Complex II activity, antimycin-sensitive Complex III activity, NaN3-sensitive Complex IV activity, and oxaloacetate-dependent citrate synthase activity, mitochondria were incubated with substrate and the absorbance was monitored using a SpectraMax iD3 Microplate Reader (Molecular Devices, CA).

2.12 | Determining the Pathogenicity

We applied the pathogenicity scoring system to evaluate the m.14687A>G mutation [36]. A variant was defined as "probably pathogenic" with a score of ≥ 11 points, "possibly pathogenic" with a score between 7 to 10 points, and a "neutral polymorphism" with a score of ≤ 6 points.

2.13 | Statistical Analysis

The student's *t*-test was used to analyze the statistical significance between two groups. A $p < 0.05$ was regarded as being of significant importance.

3 | Results

3.1 | Clinical Characteristics

We enrolled a Chinese family with maternally inherited T2DM from the Department of Endocrinology, the Fifth Affiliated Hospital of Zhengzhou University (Figure 1). The proband (III-4), aged 55years (BMI: 23kg/m [2]), visited the Fifth Affiliated Hospital of Zhengzhou University for regular treatment of diabetes. Table 1 suggested that she had mild hearing loss (55dB in the left ear and 20dB in the right ear), as well as mild visual loss (0.2 in the right eye and 0.3 in the left eye). As shown in Table 2, the HbA1c and FBG levels indicated that the patient suffered from T2DM. A family medical history showed that the patient's mother (II-4) was also a diabetic carrier. In particular, subject II-4 developed T2DM when she was 63years old, and expressed severe hearing loss (85dB in the left ear and 75dB in the right ear), and moderate visual loss (0.1 for both eyes). Furthermore, the proband's aunt (II-2) developed T2DM when she was 62; subject II-6 died from diabetic cardiomyopathy about 2years ago (Table 1).

3.2 | Identification of Pathogenic Mutations

Due to its maternal transmission, suggesting that mtDNA mutations were the important risk factors for T2DM. For this purpose, the matrilineal relatives (II-2, II-4, and III-4) and 180 control subjects were selected for mtDNA mutational analysis. PCR and direct sequencing showed the presence of a set of genetic polymorphisms belonging to human mitochondrial haplogroup G4 (Table 3) [26], there were seven mutations in the D-loop, three mutations in 12S rRNA, two mutations in 16S rRNA, one novel mutation in $tRNA^{Glu}$ (14687A>G), and a 9-bp deletion in the positions 8271 to 8279, while the remaining mutations occurred at oxidative phosphorylation (OXPHOS)-related genes. Six missense mutations were identified: *ND1* 4048G>A (p.Asp248Asn), *A6* 8701A>G (p.Thr59Ala), 8860A>G (p.Thr112Ala), 9053G>A (p.Ser176Asp), *ND3* 10398A>G (p.Thr114Ala), *ND5* 13928G>C (p.Ser54Thr) and *CytB* 15326A>G (p.Thr194Ala). These mtDNA variants were further assessed by phylogenetic analysis in mouse [37], bovine [38], and *Xenopus laevis* [39]. We found that except for the m.14687A>G mutation, other variants were not conserved (CI < 75%), suggesting that they may not be involved in T2DM progression.

By molecular level, the novel m.14687A>G mutation resided at position 60 in the TψC loop of $tRNA^{Glu}$, which was extremely conserved from various species (Figure 2A–C). Notice that the m.3291T>C mutation that also occurred at position 60 of $tRNA^{Leu(UUR)}$ was a pathogenic mutation for mitochondrial myopathy, myoclonus, and epilepsy [40, 41]. Therefore, it can be proposed that the m.14687A>G, which was similar to the m.3291T>C mutation, can also lead to mitochondrial dysfunctions that were involved in T2DM.

3.3 | The Generation of Cell Models

The lymphoblastoid cells which were derived from three T2DM patients (II-2, II-4, and III-4) harboring the m.14687A>G

TABLE 1 | Clinical and molecular features of several affected subjects with T2DM.

Subjects	Gender	Smoker	BMI (kg/m^2)	Age at test (y)	Age at onset (y)	BP (mmHg)	Ketoacidosis	PTA (Left/Right) (dB)	Level of hearing loss	Visual acuity (Left/Right)	Level of visual loss	Functional mtDNA mutations
II-2	Female	–	25	79	62	110/70	No	100/90	Profound	0.02/0.05	Severe	$tRNA^{Glu}$ 14687A>G
II-4	Female	–	27	74	63	110/70	Yes	85/75	Severe	0.1/0.1	Moderate	$tRNA^{Glu}$ 14687A>G
III-4	Female	+	23	55	49	113/86	No	55/20	Mild	0.3/0.2	Mild	$tRNA^{Glu}$ 14687A>G
III-6	Male	–	22	50	/	107/73	No	20/15	Normal	0.5/0.5	Normal	None

Abbreviations: BMI, body mass index; BP, blood pressure; dB, decibel; mtDNA, mitochondrial DNA; PTA, pure tone audiometry.

TABLE 2 | Laboratory assessments of several affected patients with T2DM.

Subjects	FBG (mmol/L)	FINS (μU/mL)	HOMA-IR	HbA1c (%)	Serum Cr (μmol/L)	eGFR (mL/min)	LDH (U/L)	ALT (U/L)	AST (U/L)	TC (mmol/L)	LDL (mmol/L)	HDL (mmol/L)
Normal range	3.9–6.1	2.6–12.0	< 2.69	4.0–6.0	57–111	80–130	50–240	9.0–50	15–40	2.85–5.70	1.31–3.37	0.9–1.95
II-2	8.0	31.0	11.02	9.2	122	55	255	16	49	3.58	4.55	0.66
II-4	7.5	4.88	1.63	6.9	110	63	268	18	55	3.11	5.10	0.81
III-4	7.0	13.90	4.32	7.5	76	95	88	29	22	4.25	3.35	1.37

Abbreviations: ALT, alanine transaminase; AST, aspartate aminotransferase; Cr, creatinine; eGFR, estimated glomerular filtration rate; FBG, fasting blood glucose; FINS, fasting insulin; HbA1c, hemoglobin A1C; HDL, high-density lipoprotein; HOMA-IR, homeostasis model assessment of IR; LDH, lactate dehydrogenase; LDL, low-density lipoprotein; TC, total cholesterol.

mutation, as well as three controls without these mutations (C-1, C-2, and C-3) were fused to a mtDNA-less human ρ°206 cells [42]. The cybrid clones were isolated by growing the fusion mixtures in selective DMEM, containing 5-bromo-2′-deoxyuridine (BrdU) and lacking uridine. PCR-Sanger sequencing revealed the occurrence of the m.14687A>G mutation in the cybrid cells.

3.4 | The Steady-State Level of $tRNA^{Glu}$ Was Decreased in 14687G Cybrids

To see whether m.14687A>G mutation affected tRNA stability levels, we used Northern Blotting to test the steady-state levels of $tRNA^{Glu}$, $tRNA^{Met}$ and $tRNA^{Cys}$ in six cybrid cells. As shown in Figure 3, this mtDNA mutation caused approximately 52% reductions in $tRNA^{Glu}$ stability level ($p < 0.001$), whereas the steady-state levels of $tRNA^{Met}$ and $tRNA^{Cys}$ were not affected in either 14687A or 14687G cybrids ($p = 0.0783$ and 0.2367, respectively).

3.5 | mtDNA Copy Number Dropped in Patients With m.14687A>G Mutation

Since mtDNA copy number was a biomarker for mitochondrial functions, we next evaluated the peripheral blood mtDNA content in patients and controls with and without the m.14687A>G mutation. As shown in Figure 4A, we found that there was approximately a 43.5% reduction in subjects with this mutation, as compared with controls ($p = 0.0024$).

3.6 | ATP Production Was Decreased in 14687G Cybrids

As shown in Figure 4B, the average ATP production in 14687G cybrids was 36.5%, which was related to the mean value measured in 14687A cybrids ($p = 0.0042$).

3.7 | MMP Decreased in 14687G Cybrids

MMP was an important component in the process of energy storage during OXPHOS, which was an early event for apoptosis [43]. As shown in Figure 4C, the average MMP levels in 14687G cybrids were 62.6% of the mean value measured in 14687A cybrids ($p = 0.0007$).

3.8 | Enhanced of ROS Levels in 14687G Cybrids

The ROS levels were determined using fluorometry. We found that, compared with 14687A cybrids (Figure 4D), an approximately 47.6% increase in ROS production was observed in 14687G cybrids ($p = 0.0011$, Figure 5).

3.9 | The m.14687A>G Mutation Inhibited Complex I and Complex IV Activities in Cells

We further examined the enzymatic activities of Complexes I~IV in cybrids with and without this mutation (Figure 5). The

TABLE 3 | mtDNA variants in this Chinese pedigree with T2DM.

Genes	Position	Replacement	Conservation (H/B/M/X)[a]	rCRS[b]	Previously reported[c]
D-loop	73	A to G		A	Yes
	153	A to G		A	Yes
	263	A to G		A	Yes
	310	T to CTC/TC		T	Yes
	524	Del C		C	Yes
	16,183	T to C		T	Yes
	16,189	T to C		T	Yes
12S rRNA	709	G to A	G/G/A/–	G	Yes
	750	A to G	A/A/A/–	A	Yes
	1438	A to G	A/A/A/G	A	Yes
16S rRNA	2706	A to G	A/G/A/A	A	Yes
	3107	DelN		N	Yes
ND1	3552	T to A		T	Yes
	3970	C to T		C	Yes
	4048	G to A (Asp to Asn)		G	Yes
	4071	C to T		C	Yes
ND2	4715	A to G		A	Yes
	4769	A to G		A	Yes
	4883	C to T		C	Yes
CO1	6053	C to T		C	Yes
	7028	C to T		C	Yes
CO_2	8020	G to A		G	Yes
NC7	8271–8279	Del 9-bp		9-bp	Yes
A6	8701	A to G (Thr to Ala)	T/S/L/Q	A	Yes
	8860	A to G (Thr to Ala)	T/A/A/T	A	Yes
CO3	9540	T to C		T	Yes
ND3	10,310	G to A		G	Yes
	10,398	A to G (Thr to Ala)	T/T/T/A	A	Yes
	10,400	C to T		C	Yes
ND4	10,873	T to C		T	Yes
	11,719	G to A		G	Yes
ND5	12,705	C to T		C	Yes
	13,928	G to C (Ser to Thr)		G	Yes
$tRNA^{Glu}$	14,687	A to G	A/A/A/A	A	No
ND6	14,668	C to T		C	Yes
CytB	14,783	T to C		T	Yes
	15,301	G to A		G	Yes
	15,326	A to G (Thr to Ala)	T/M/I/I	A	Yes

[a]Conservation assessment of tRNA, rRNA, and OXPHOS encoding gene mutations in Human (H), Bovine (B), Mouse (M) and *Xenopus Laevis* (X).
[b]rCRS: reversed Cambridge Reference Sequences.
[c]Please see the online Mitomap (www.mitomap.org) and mtDB (http://www.mtdb.igp.uu.se/) databases.

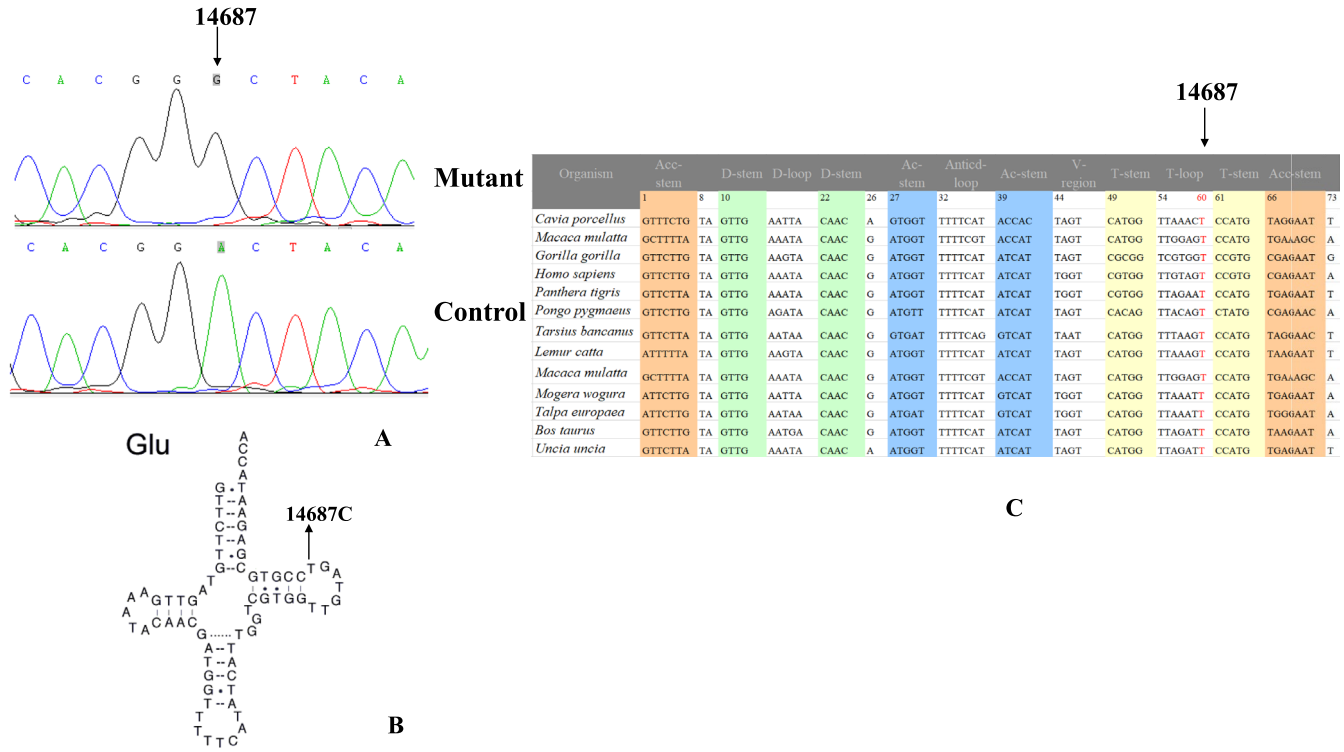

Organism	Acc-stem		D-stem	D-loop	D-stem		Ac-stem	Anticd-loop	Ac-stem	V-region	T-stem	T-loop	T-stem	Acc-stem	
	1	8	10		22	26	27	32	39	44	49	54 60	61	66	73
Cavia porcellus	GTTTCTG	TA	GTTG	AATTA	CAAC	A	GTGGT	TTTTCAT	ACCAC	TAGT	CATGG	TTAAACT	CCATG	TAGGAAT	T
Macaca mulatta	GCTTTTA	TA	GTTG	AAATA	CAAC	G	ATGGT	TTTTCGT	ACCAT	TAGT	CATGG	TTGGAGT	CCATG	TGAAAGC	A
Gorilla gorilla	GTTCTTG	TA	GTTG	AAGTA	CAAC	G	ATGGT	TTTTCAT	ATCAT	TAGT	CGCGG	TCGTGGT	CCGTG	CGAGAAT	G
Homo sapiens	GTTCTTG	TA	GTTG	AAATA	CAAC	G	ATGGT	TTTTCAT	ATCAT	TGGT	CGTGG	TTGTAGT	CCGTG	CGAGAAT	A
Panthera tigris	GTTCTTA	TA	GTTG	AAATA	CAAC	G	ATGGT	TTTTCAT	ATCAT	TGGT	CGTGG	TTAGAAT	CCATG	TGAGAAT	T
Pongo pygmaeus	GTTCTTG	TA	GTTG	AGATA	CAAC	G	ATGTT	TTTTCAT	ATCAT	TAGT	CACAG	TTACAGT	CTATG	CGAGAAC	A
Tarsius bancanus	GTTCTTA	TA	GTTG	AATAA	CAAC	G	GTGAT	TTTTCAG	GTCAT	TAAT	CATGG	TTTAAGT	CCATG	TAGGAAC	T
Lemur catta	ATTTTTA	TA	GTTG	AAGTA	CAAC	G	ATGGT	TTTTCAT	ATCAT	TAGT	CATGG	TTAAAGT	CCATG	TAAGAAT	T
Macaca mulatta	GCTTTTA	TA	GTTG	AAATA	CAAC	G	ATGGT	TTTTCGT	ACCAT	TAGT	CATGG	TTGGAGT	CCATG	TGAAAGC	A
Mogera wogura	ATTCTTG	TA	GTTG	AATTA	CAAC	G	ATGGT	TTTTCAT	GTCAT	TGGT	CATGG	TTAAATT	CCATG	TGAGAAT	A
Talpa europaea	ATTCTTG	TA	GTTG	AATAA	CAAC	G	ATGAT	TTTTCAT	GTCAT	TGGT	CATGG	TTAAATT	CCATG	TGGGAAT	A
Bos taurus	GTTCTTG	TA	GTTG	AATGA	CAAC	G	ATGGT	TTTTCAT	ATCAT	TAGT	CATGG	TTAGATT	CCATG	TAAGAAT	A
Uncia uncia	GTTCTTA	TA	GTTG	AAATA	CAAC	A	ATGGT	TTTTCAT	ATCAT	TAGT	CATGG	TTAGATT	CCATG	TGAGAAT	T

FIGURE 2 | Molecular characterization of T2DM associated mt-tRNA^{Glu} mutation. (A) Identification of m.14687A>G mutation by direct sequencing. (B) Cloverleaf structure of tRNA^{Glu} gene, arrow indicated the m.14687A>G mutation. (C) Alignment of tRNA^{Glu} gene from different species, arrow denoted the position 60, corresponding to the m.14687A>G mutation.

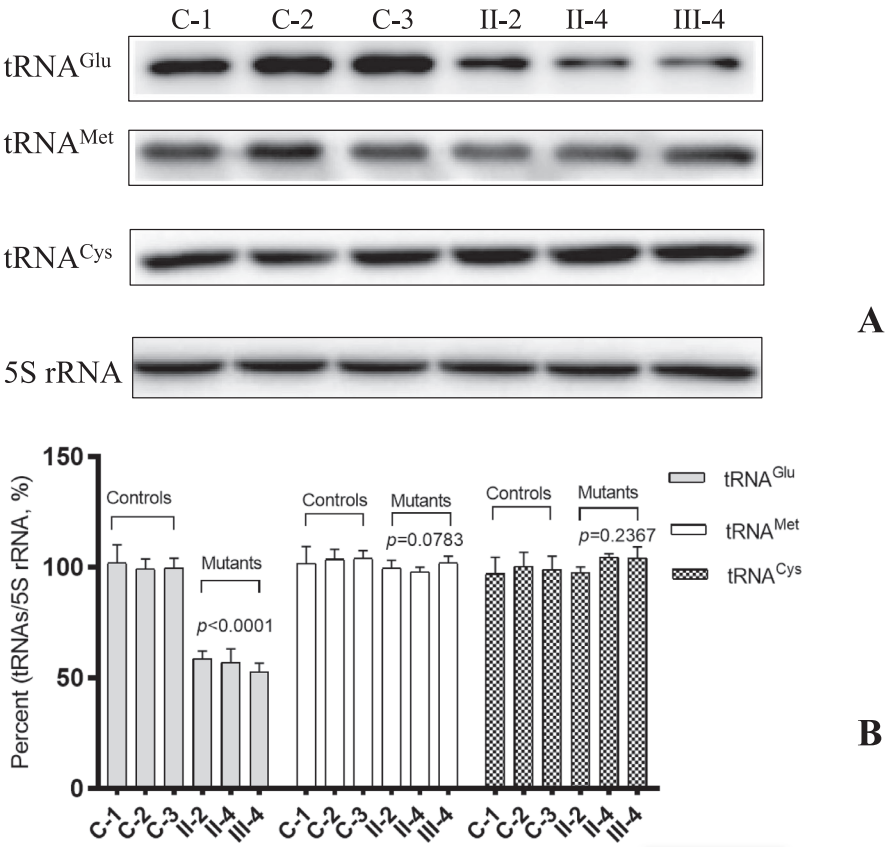

FIGURE 3 | Analysis of mt-tRNA steady-state levels. (A) 2 μg mt-tRNA were electrophoresed through a denaturing polyacrylamide gel and hybridized with DIG-labeled oligonucleotide probes for mt-tRNA^{Glu}, mt-tRNA^{Met}, and mt-tRNA^{Cys} and 5S rRNA. (B) Qualification of mt-tRNA levels.

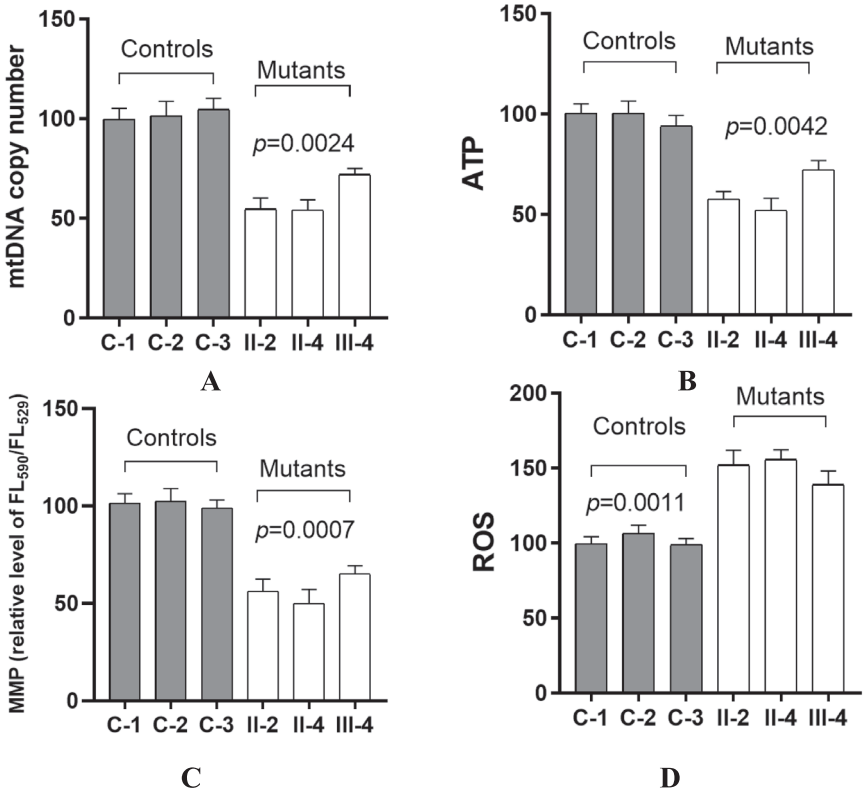

FIGURE 4 | Assessments of mitochondrial functions in mutant and control cell lines. (A) mtDNA copy number; (B) ATP analysis; (C) MMP analysis; (D) ROS qualification.

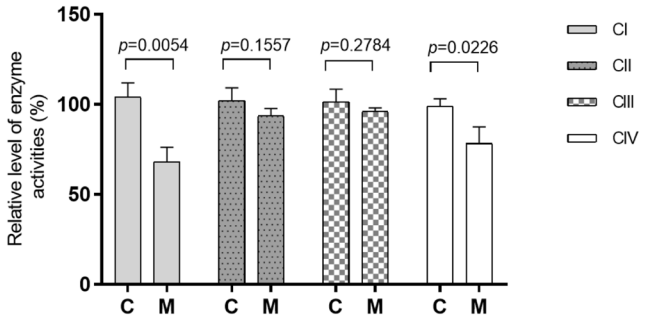

FIGURE 5 | Analysis of enzymatic activities of mitochondrial respiratory chain complexes in three cybrids with m.14687A>G mutation and three control cell lines without this mutation. C: Control group; M: Mutant group.

activities of Complex I and Complex IV were markedly inhibited ($p = 0.0054$ and 0.0226, respectively) in 14687G cybrids, while the Complex II and Complex III enzyme activities were not affected ($p = 0.1557$ and 0.2784, respectively) in either 14687G cybrids or 14687A cybrids.

3.10 | The m.14687A>G Was a "Definitely Pathogenic" Mutation for T2DM

Based on the pathogenicity scoring system, the total scores of m.14687A>G mutation were 11 points and can be classified as "definitely pathogenic" (Table 4).

4 | Discussion

In the present study, we investigated the pathogenic role of a novel m.14687A>G mutation at genetic, molecular, and biochemical levels. Interestingly, T2DM only affects matrilineal relatives of this pedigree, highlighting the importance of mtDNA mutations to this disorder. The age of diabetes onset in this family ranges from 49 to 63 years, with an average age of 58. Among the family members, three subjects suffered from deafness, DM, and visual impairments. The family members in this family had an earlier age of diabetes onset, indicating that mtDNA mutations may serve as risk factors for early detection of this disease.

Mutations analysis revealed the existence of a novel m.14687A>G, which was only found in matrilineal relatives but absent in controls. By molecular level, the m.14687A>G mutation occurred at an extremely conserved nucleotide in the TψC loop of $tRNA^{Glu}$, a position that was important for tRNA structure and functions. Interestingly, the well-known m.3291 T>C mutation, which was also located at the same position of $tRNA^{Leu(UUR)}$, had been regarded as a pathogenic mutation for mitochondrial myopathy [40, 41]. Thus, it can be speculated that the m.14687A>G mutation, which was similar to the m.3291 T>C mutation, may also cause the mitochondrial dysfunctions that were involved in T2DM progression.

Trans-mitochondrial technology was frequently used to assess the contribution of mtDNA genetic polymorphisms to OXPHOS function since noise from the nuclear genetic background was

TABLE 4 | The pathogenic role of m.14687A>G mutation.

Scoring criteria	m.14687A>G mutation	Score/20	Classification
More than one independent report	No	0	≤6 points: neutral polymorphisms; 7–10 points: possibly pathogenic; ≥11 points (including evidence from single fiber, steady-state level or trans-mitochondrial cybrid studies): definitely pathogenic
Evolutionary conservation of the base pair	No changes	2	
Variant heteroplasmy	No	0	
Segregation of the mutation with disease	Yes	2	
Biochemical defect in complex I, III or IV	Yes	2	
Evidence of mutation segregation with biochemical defect from single fiber studies	No evidence	0	
Mutant mt-tRNA steady-state level or evidence of pathogenicity in trans-mitochondrial cybrid studies	Strong evidence	5	
Maximum score	Definitely pathogenic	11	

adjusted. In the current study, we established three mutant cell lines with this mutation and three control cells without this mtDNA mutation. Compared with 14687A cybrid, the 14687G cybrid showed approximately 52% reductions in the steady-state level of $tRNA^{Glu}$, which was below the proposed threshold to produce a clinical phenotype associated with a tRNA mutation [44], nevertheless, the m.14687A>G mutation did not alter the steady-state levels of $tRNA^{Met}$ and $tRNA^{Cys}$. Thus, a failure in tRNA metabolism caused by the m.14687A>G mutation may lead to the impairment of respiratory chain functions, as in the case of the $tRNA^{Leu(UUR)}$ 3243A>G mutation [45]. As a result, the aberrant mt-tRNA metabolism reduced the activities of CI and CIV in mutant cells, which were consistent with the clinical phenotypes of the affected individuals.

We found that mutant cells exhibited more severe mitochondrial dysfunction, and the mtDNA copy number, ATP, MMP were markedly decreased in mutant cells, whereas the levels of ROS increased significantly. Indeed, the mtDNA copy number was an essential indicator of the normal functioning of the mitochondria, which reflected mitochondrial biogenesis [46]. MMP is essential for the maintenance of cellular health and viability, and the loss of MMP is implicated in cell apoptosis and decreased ATP production [47]. Thus, the abnormal MMP may lead to an increase in ROS production. ROS were the by-products of oxidative stress, and include peroxides, superoxides, hydroxyl radicals, and singlet oxygen [48]. High ROS concentration may react with proteins, lipids, RNA, or DNA, and frequently lead to irreversible functional alterations, including regulating apoptosis, impairing insulin signaling pathway, and contributing to T2DM progression [49, 50].

In conclusion, our study suggested that the novel $tRNA^{Glu}$ 14687A>G mutation was associated with T2DM. Furthermore, the incomplete penetrance of T2DM and variable clinical phenotypes indicate that the m.14687A>G mutation was not sufficient to produce clinical phenotypes. Therefore, other factors, such as environmental factors, nuclear genes, or epigenetic modification, may contribute to T2DM progression. Thus, our study provides novel insights into the molecular mechanisms, early detection, and prevention of mitochondrial diabetes.

Author Contributions

Xiaojuan Rao and Liran Xie conceived and designed the experiments, analyzed the data, and wrote the manuscript. Shuangwei Shi and Yifan Fang collected the samples. All authors contributed to the article and approved the submitted version.

Disclosure

The authors have nothing to report.

Ethics Statement

The study was approved by the Ethics Committee of Fifth Affiliated Hospital of Zhengzhou University (Approval Number: KY2023088-KO2).

Consent

All participants signed informed consent in accordance with the Declaration of Helsinki.

Conflicts of Interest

The authors declare no conflicts of interest.

Data Availability Statement

The data that support the findings of this study are available from the corresponding author upon reasonable request.

References

1. Y. Xu, L. Wang, J. He, et al., "Prevalence and Control of Diabetes in Chinese Adults," *JAMA* 310, no. 9 (2013): 948–959, https://doi.org/10.1001/jama.2013.168118.

2. A. D. Stockwell, M. C. Chang, A. Mahajan, et al., "Multi-Ancestry GWAS Analysis Identifies Two Novel Loci Associated With Diabetic Eye Disease and Highlights APOL1 as a High Risk Locus in Patients With Diabetic Macular Edema," *PLoS Genetics* 19 (2023): e1010609, https://doi.org/10.1371/journal.pgen.1010609.

3. J. Szendroedi, E. Phielix, and M. Roden, "The Role of Mitochondria in Insulin Resistance and Type 2 Diabetes Mellitus," *Nature Reviews. Endocrinology* 8 (2011): 92–103, https://doi.org/10.1038/nrendo.2011.138.

4. K. F. Petersen, D. Befroy, S. Dufour, et al., "Mitochondrial Dysfunction in the Elderly: Possible Role in Insulin Resistance," *Science* 300 (2003): 1140–1142, https://doi.org/10.1126/science.1082889.

5. W. I. Sivitz and M. A. Yorek, "Mitochondrial Dysfunction in Diabetes: From Molecular Mechanisms to Functional Significance and Therapeutic Opportunities," *Antioxidants & Redox Signaling* 12 (2010): 537–577, https://doi.org/10.1089/ars.2009.2531.

6. H. Song, J. Lee, Y. Lee, S. Kim, and S. Kang, "Reactive Oxygen Species as a Common Pathological Link Between Alcohol Use Disorder and Alzheimer's Disease With Therapeutic Implications," *International Journal of Molecular Sciences* 26 (2025): 3272, https://doi.org/10.3390/ijms26073272.

7. K. L. Hoehn, A. B. Salmon, C. Hohnen-Behrens, et al., "Insulin Resistance Is a Cellular Antioxidant Defense Mechanism," *Proceedings of the National Academy of Sciences of the United States of America* 106 (2009): 17787–17792, https://doi.org/10.1073/pnas.0902380106.

8. A. Tirosh, R. Potashnik, N. Bashan, and A. Rudich, "Oxidative Stress Disrupts Insulin-Induced Cellular Redistribution of Insulin Receptor Substrate-1 and Phosphatidylinositol 3-Kinase in 3T3-L1 Adipocytes. A Putative Cellular Mechanism for Impaired Protein Kinase B Activation and GLUT4 Translocation," *Journal of Biological Chemistry* 274 (1999): 10595–10602, https://doi.org/10.1074/jbc.274.15.10595.

9. A. Rudich, A. Tirosh, R. Potashnik, R. Hemi, H. Kanety, and N. Bashan, "Prolonged Oxidative Stress Impairs Insulin-Induced GLUT4 Translocation in 3T3-L1 Adipocytes," *Diabetes* 47 (1998): 1562–1569, https://doi.org/10.2337/diabetes.47.10.1562.

10. J. A. Maassen, L. M. 'T Hart, E. Van Essen, et al., "Mitochondrial Diabetes: Molecular Mechanisms and Clinical Presentation," *Diabetes* 53, no. Suppl 1 (2004): S103–S109, https://doi.org/10.2337/diabetes.53.2007.s103.

11. J. Fujikura, K. Nakao, M. Sone, et al., "Induced Pluripotent Stem Cells Generated From Diabetic Patients With Mitochondrial DNA A3243G Mutation," *Diabetologia* 55 (2012): 1689–1698, https://doi.org/10.1007/s00125-012-2508-2.

12. J. M. van den Ouweland, H. H. Lemkes, W. Ruitenbeek, et al., "Mutation in Mitochondrial tRNALeu(UUR) Gene in a Large Pedigree With Maternally Transmitted Type II Diabetes Mellitus and Deafness," *Nature Genetics* 1, no. 5 (1992): 368–371, https://doi.org/10.1038/ng0892-368.

13. H. Liu, R. Li, W. Li, et al., "Maternally Inherited Diabetes Is Associated With a Homoplasmic T10003C Mutation in the Mitochondrial tRNA(Gly) Gene," *Mitochondrion* 21 (2015): 49–57, https://doi.org/10.1016/j.mito.2015.01.004.

14. K. Li, L. Wu, J. Liu, W. Lin, Q. Qi, and T. Zhao, "Maternally Inherited Diabetes Mellitus Associated With a Novel m.15897G>A Mutation in Mitochondrial tRNAThr Gene," *Journal Diabetes Research* 2020 (2020): 2057187, https://doi.org/10.1155/2020/2057187.

15. L. Yang, Q. Guo, J. Leng, K. Wang, and Y. Ding, "Late Onset of Type 2 Diabetes Is Associated With Mitochondrial tRNATrp A5514G and tRNASer(AGY) C12237T Mutations," *Journal of Clinical Laboratory Analysis* 36, no. 1 (2022): e24102, https://doi.org/10.1002/jcla.24102.

16. D. C. Wallace, "A Mitochondrial Paradigm of Metabolic and Degenerative Diseases, Aging, and Cancer: A Dawn for Evolutionary Medicine," *Annual Review of Genetics* 39 (2005): 359–407, https://doi.org/10.1146/annurev.genet.39.110304.095751.

17. American Diabetes Association, "Diagnosis and Classification of Diabetes Mellitus," *Diabetes Care* 33 (2010): S62–S69.

18. J. A. Levine, "Obesity in China: Causes and Solutions," *Chinese Medical Journal* 121 (2008): 1043–1050.

19. L. Lin, P. Cui, Z. Qiu, et al., "The Mitochondrial tRNAAla 5587T>C and tRNALeu(CUN) 12280A>G Mutations May Be Associated With Hypertension in a Chinese Family," *Experimental and Therapeutic Medicine* 17 (2019): 1855–1862, https://doi.org/10.3892/etm.2018.7143.

20. D. Jones, J. Basile, W. Cushman, et al., "Managing Hypertension in the Southeastern United States: Applying the Guidelines From the Sixth Report of the Joint National Committee on Prevention, Detection, Evaluation, and Treatment of High Blood Pressure (JNC VI)," *American Journal of the Medical Sciences* 318 (1999): 357–364.

21. X. Yu, S. Li, and Y. Ding, "Maternally Transmitted Nonsyndromic Hearing Impairment May Be Associated With Mitochondrial tRNAAla 5601C>T and tRNALeu(CUN) 12311T>C Mutations," *Journal of Clinical Laboratory Analysis* 36 (2022): e24298, https://doi.org/10.1002/jcla.24298.

22. H. X. Gong, B. Wu, S. Y. Xie, W. Zhang, and S. Chen, "OCTA Characteristics in Non-Arteritic Central Retinal Artery Occlusion and Correlation With Visual Acuity," *International Journal of Ophthalmology* 17, no. 2 (2024): 289–296, https://doi.org/10.18240/ijo.2024.02.10.

23. X. Zhou and J. Xu, "Association Between Serum Uric Acid-To-High-Density Lipoprotein Cholesterol Ratio and Insulin Resistance in Patients With Type 2 Diabetes Mellitus," *Journal of Diabetes Investigation* 15 (2024): 113–120, https://doi.org/10.1111/jdi.14086.

24. L. Wu, R. Li, J. Chen, Y. Chen, M. Yang, and Q. Wu, "Analysis of Mitochondrial A1555G Mutation in Infants With Hearing Impairment," *Experimental and Therapeutic Medicine* 15 (2018): 5307–5313, https://doi.org/10.3892/etm.2018.6078.

25. R. M. Andrews, I. Kubacka, P. F. Chinnery, R. N. Lightowlers, D. M. Turnbull, and N. Howell, "Reanalysis and Revision of the Cambridge Reference Sequence for Human Mitochondrial DNA," *Nature Genetics* 23 (1999): 147, https://doi.org/10.1038/13779.

26. Q. P. Kong, H. J. Bandelt, C. Sun, et al., "Updating the East Asian mtDNA Phylogeny: A Prerequisite for the Identification of Pathogenic Mutations," *Human Molecular Genetics* 15 (2006): 2076–2086, https://doi.org/10.1093/hmg/ddl130.

27. Z. Jiang, L. Teng, S. Zhang, and Y. Ding, "Mitochondrial ND1 T4216C and ND2 C5178A Mutations Are Associated With Maternally Transmitted Diabetes Mellitus," *Mitochondrial DNA Part A DNA Mapping, Sequencing, and Analysis* 32 (2021): 59–65, https://doi.org/10.1080/24701394.2020.1856101.

28. E. Ruiz-Pesini and D. C. Wallace, "Evidence for Adaptive Selection Acting on the tRNA and rRNA Genes of Human Mitochondrial DNA," *Human Mutation* 27 (2006): 1072–1081, https://doi.org/10.1002/humu.20378.

29. H. Li, J. Geng, H. Yu, X. Tang, X. Yang, and L. Xue, "Mitochondrial tRNAThr 15909A>G Mutation Associated With Hypertension in a Chinese Han Pedigree," *Biochemical and Biophysical Research Communications* 495 (2018): 574–581, https://doi.org/10.1016/j.bbrc.2017.11.061.

30. C. Xu, L. Tong, J. Rao, et al., "Heteroplasmic and Homoplasmic m.616T>C in Mitochondria tRNAPhe Promote Isolated Chronic Kidney Disease and Hyperuricemia," *JCI Insight* 7 (2022): e157418, https://doi.org/10.1172/jci.insight.157418.

31. X. Yu, S. Li, Q. Guo, J. Leng, and Y. Ding, "The Association Between Mitochondrial tRNAGlu Variants and Hearing Loss: A Case-Control Study," *Pharmacogenomics and Personalized Medicine* 17 (2024): 77–89, https://doi.org/10.2147/PGPM.S441281.

32. S. Gong, Y. Peng, P. Jiang, et al., "A Deafness-Associated tRNA-His Mutation Alters the Mitochondrial Function, ROS Production and Membrane Potential," *Nucleic Acids Research* 42, no. 12 (2014): 8039–8048, https://doi.org/10.1093/nar/gku466.

33. Y. Ding, B. H. Xia, C. J. Zhang, and G. C. Zhuo, "Mitochondrial tRNALeu(UUR) C3275T, tRNAGln T4363C and tRNALys A8343G Mutations May Be Associated With PCOS and Metabolic Syndrome," *Gene* 642 (2018): 299–306, https://doi.org/10.1016/j.gene.2017.11.049.

34. P. Jiang, M. Liang, C. Zhang, et al., "Biochemical Evidence for a Mitochondrial Genetic Modifier in the Phenotypic Manifestation of Leber's Hereditary Optic Neuropathy-Associated Mitochondrial DNA Mutation," *Human Molecular Genetics* 25 (2016): 3613–3625, https://doi.org/10.1093/hmg/ddw199.

35. W. Fan, J. Zheng, W. Kong, et al., "Contribution of a Mitochondrial Tyrosyl-tRNA Synthetase Mutation to the Phenotypic Expression of the Deafness-Associated tRNASer(UCN) 7511A>G Mutation," *Journal of Biological Chemistry* 294 (2019): 19292–19305, https://doi.org/10.1074/jbc.RA119.010598.

36. J. W. Yarham, M. Al-Dosary, E. L. Blakely, et al., "A Comparative Analysis Approach to Determining the Pathogenicity of Mitochondrial tRNA Mutations," *Human Mutation* 32 (2011): 1319–1325, https://doi.org/10.1002/humu.21575.

37. M. J. Bibb, R. A. Van Etten, C. T. Wright, et al., "Sequence and Gene Organization of Mouse Mitochondrial DNA," *Cell* 26 (1981): 167–180.

38. G. Gadaleta, G. Pepe, G. De Candia, et al., "The Complete Nucleotide Sequence of the *Rattus norvegicus* Mitochondrial Genome: Cryptic Signals Revealed by Comparative Analysis Between Vertebrates," *Journal of Molecular Evolution* 28 (1989): 497–516, https://doi.org/10.1007/BF02602930.

39. B. A. Roe, D. P. Ma, R. K. Wilson, and J. F. Wong, "The Complete Nucleotide Sequence of the *Xenopus laevis* Mitochondrial Genome," *Journal of Biological Chemistry* 260 (1985): 9759–9774.

40. Y. Sunami, K. Sugaya, N. Chihara, Y. I. Goto, and S. Matsubara, "Variable Phenotypes in a Family With Mitochondrial Encephalomyopathy Harboring a 3291T >C Mutation in Mitochondrial DNA," *Neurological Sciences* 32 (2011): 861–864, https://doi.org/10.1007/s10072-011-0719-9.

41. G. Uziel, F. Carrara, T. Granata, et al., "Neuromuscular Syndrome Associated With the 3291T–>C Mutation of Mitochondrial DNA: A Second Case," *Neuromuscular Disorders* 10 (2000): 415–418, https://doi.org/10.1016/s0960-8966(99)00115-7.

42. M. P. King and G. Attadi, "Mitochondria-Mediated Transformation of Human Rho(0) Cells," *Methods in Enzymology* 264 (1996): 313–334, https://doi.org/10.1016/s0076-6879(96)64030-0.

43. L. D. Zorova, V. A. Popkov, E. Y. Plotnikov, et al., "Mitochondrial Membrane Potential," *Analytical Biochemistry* 552 (2018): 50–59, https://doi.org/10.1016/j.ab.2017.07.009.

44. X. Chen, F. Meng, C. Chen, et al., "Deafness-Associated tRNAPhe Mutation Impaired Mitochondrial and Cellular Integrity," *Journal of Biological Chemistry* 300 (2024): 107235, https://doi.org/10.1016/j.jbc.2024.107235.

45. D. S. Lin, Y. W. Huang, C. S. Ho, et al., "Impact of Mitochondrial A3243G Heteroplasmy on Mitochondrial Bioenergetics and Dynamics of Directly Reprogrammed MELAS Neurons," *Cells* 12 (2022): 15, https://doi.org/10.3390/cells12010015.

46. W. Sun, C. R. Zeng, D. Yue, and Y. C. Hu, "Involvement of Mitochondrial Dysfunction in Hepatotoxicity Induced by *Ageratina adenophora* in Mice," *Journal of Zhejiang University. Science. B* 20 (2019): 693–698, https://doi.org/10.1631/jzus.B1800645.

47. Y. Chen, S. Chen, H. Liang, et al., "Bcl-2 Protects TK6 Cells Against Hydroquinone-Induced Apoptosis Through PARP-1 Cytoplasm Translocation and Stabilizing Mitochondrial Membrane Potential," *Environmental and Molecular Mutagenesis* 59 (2018): 49–59, https://doi.org/10.1002/em.22126.

48. B. D'Autréaux and M. B. Toledano, "ROS as Signalling Molecules: Mechanisms That Generate Specificity in ROS Homeostasis," *Nature Reviews. Molecular Cell Biology* 8 (2007): 813–824, https://doi.org/10.1038/nrm2256.

49. K. Brieger, S. Schiavone, F. J. Miller, Jr., and K. H. Krause, "Reactive Oxygen Species: From Health to Disease," *Swiss Medical Weekly* 142 (2012): w13659, https://doi.org/10.4414/smw.2012.13659.

50. K. M. Abu Khadra, M. I. Bataineh, A. Khalil, and J. Saleh, "Oxidative Stress and Type 2 Diabetes: The Development and the Pathogenesis, Jordanian Cross-Sectional Study," *European Journal of Medical Research* 29 (2024): 370, https://doi.org/10.1186/s40001-024-01906-4.